Journal of Thermal Analysis and Calorimetry, Vol. 90 (2007) 3, 673–679

THERMAL PROPERTIES, INDUCTION PERIOD, INTERFACIAL ENERGY AND NUCLEATION PARAMETERS OF SOLUTION GROWN BENZOPHENONE

*G. Madhurambal[1], P. Ramasamy[2], P. AnbuSrinivasan[3] and S. C. Mojumdar[4,5]**

[1]Departmant of Chemistry, ADM College for Women, Nagapattinam, TamilNadu, India
[2]Crystal Growth Centre, Anna University, Chennai, India
[3]Department of Chemistry, AVC College, Mayiladuthurai, TamilNadu, India
[4]Department of Chemical Engineering, University of Waterloo, 200 University Ave. West, Waterloo, ON, N2L 3G1, Canada
[5]University of New Brunswick, Saint John, NB, E2L 4L5, Canada

Benzophenone is a well-known material, which exhibits non-linear optical (NLO) property. It has been grown by solution technique adopting slow evaporation method from solvents $CHCl_3$, CCl_4 for the first time. Solubility metastable zone width and inductions periods of benzophenone in $CHCl_3$ and CCl_4 were determined. Interfacial tension values at two different temperatures for various super saturations, such as 1.10, 1.15, 1.20 and 1.25 were determined using induction period. From interfacial tension values, the nucleation parameters, such as the radius of the critical nuclei (r^*), the free energy change for the formation of a critical nucleus (ΔG^*) and the number of molecules in the critical nucleus were also calculated for benzophenone in $CHCl_3$ and CCl_4 at two different temperature. The effect of surface tension, viscosity, density of these solvents are correlated with interfacial tension. The metastable zone width is also correlated with interfacial tension. The solution grown crystals were carefully harvested and subjected to various characterization studies to check its purity and to determine its applicability.

Keywords: *benzophenone, characterization studies, interfacial tension, nucleation parameters, solution technique*

Introduction

Many organic materials have been found to have greater non-linear optoelectrical properties than inorganic substances [1–3]. Organic single crystals possess unique optoelectronic properties because organic molecules have delocalized electrons, namely, conjugated electron systems exhibit various photo responses such as photoconductive, photo voltaic, photo catalytic behavior and so on. Benzophenone is a well-known example of organic material, which exhibits NLO property. This can be grown from melt [4–6]. There are several reports available in the literature for the growth of benzophenone by various methods viz. Czochralski technique [4], under-cooled method [7], solution method [8], and Bridgman Technique [9]. The non-linear optical property of benzophenone and its derivatives have been studied using powder second harmonic generation (SHG) method. Their results show several of these compounds generate SHG signals stronger than that of urea [10, 11]. There are several reports available in literature on the growth of benzophenone by adopting above methods.

Many authors investigated organic and organometallic compounds due to their chemical, biological and environmental importants and examined their various properties [12–37]. In our previous papers, we described the thermoanalytical properties of various organic and organometallic compounds [38–65]. In the present study, investigations have been made to evaluate the interfacial tension (γ) between benzophenone and $CHCl_3$ based solution by measuring the induction period and hence to calculate the critical radius (r^*), number of molecules in the critical nucleus (i^*) and Gibb's free energy (ΔG^*) for the formation of a critical nucleus of benzophenone grown from $CHCl_3$ solution. The similar investigations have also been carried out between benzophenone and CCl_4. Recently Arivanandhan *et al.* [66] reported the growth of benzophenone using vertical Bridgman– Stockbarger system.

Experimental

Growth of benzophenone

The analar benzophenone was re-crystallized from $CHCl_3$ for several times. The solubility of benzophenone in $CHCl_3$ and CCl_4 were determined in various temperatures. Solubility determination shows that the solubility increases with temperature. Figures 1 and 2 show that the solubility increases with temperature increase.

* Author for correspondence: smojumda@engmail.uwaterloo.ca, scmojumdar@hotmail.com

1388–6150/$20.00

Akadémiai Kiadó, Budapest, Hungary
Springer, Dordrecht, The Netherlands

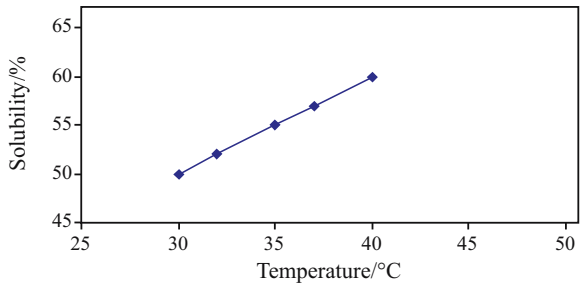

Fig. 1 Solubility of benzophenone in $CHCl_3$

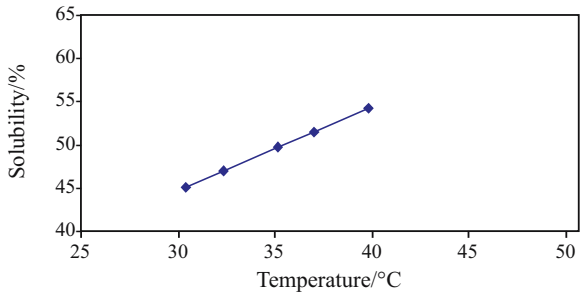

Fig. 2 Solubility of benzophenone in CCl_4

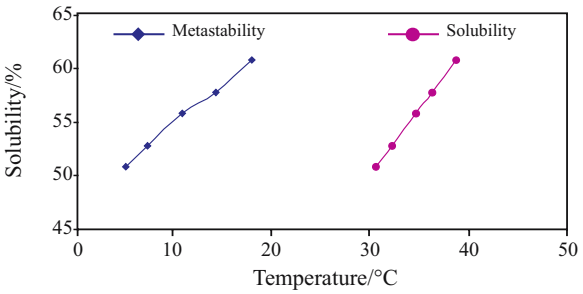

Fig. 3 Metastable zone width of benzophenone in $CHCl_3$

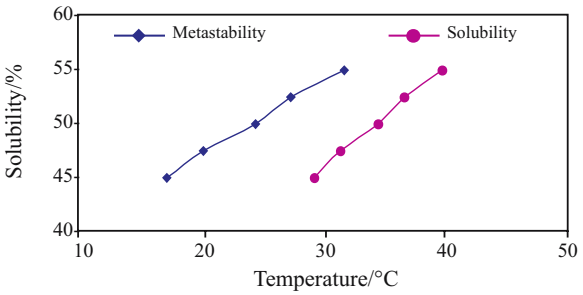

Fig. 4 Metastable zone width of benzophenone in CCl_4

Metastable zone width determination

After solubility determination, the metastable zone width of benzophenone in $CHCl_3$ and CCl_4 were determined. Saturated solutions of benzophenone in $CHCl_3$ at different temperatures were allowed for systematic slow cooling. The temperature at which the first nucleation was observed corresponds to their width of metastable zone. The metastable zone width of benzophenone in $CHCl_3$ has been shown in Fig. 3 and given in Table 1. The metastable zone width of benzophenone in CCl_4 was also determined by the same procedure and has been shown in Fig. 4 and the data have been given in Table 2. The metastable zone width of benzophenone depends on solvent nature. Benzophenone, a ketone compound has higher solubility in $CHCl_3$ and CCl_4 than the solubility of anthracene, a polynuclear aromatic hydrocarbon. A higher metastable zone width is observed in $CHCl_3$ solvent than CCl_4. The re-crystallized sample of benzophenone was dissolved in $CHCl_3$ and CCl_4 and the solutions were allowed for slow evaporation. The grown crystals were subjected to various characterization studies, such as UV, FTIR, ^{1}HNMR, TG and DTA. Thermal studies show the purity of benzophenone. FTIR and ^{1}HNMR studies show the presence of functional groups.

Table 1 Nucleation temperature and metastable zone width of benzophenone in $CHCl_3$

Saturation temperature/°C	Nucleation temperature/°C	Meta-stable zone width/°C
30	5.5	24.5
32	8.2	23.8
35	12.6	22.4
37	16.8	20.2
40	21.2	18.8

Table 2 Nucleation temperature and metastable zone width of benzophenone in CCl_4

Saturation temperature/°C	Nucleation temperature/°C	Metastable zone width/°C
30	15.5	14.5
32	21.3	10.7
35	25.4	9.6
37	28.2	8.8
40	32.3	7.7

Determination of induction period, interfacial energies and nucleation parameters

There are several methods of measuring the induction period depending upon the solubility of the materials. Here, the visual observation method has been followed. Solutions of benzophenone in $CHCl_3$ at different super saturation values were prepared and subjected to systematic slow evaporation. The time period that elapses between the achievement of super saturation and appearance of visible nuclei is taken as the induction period (τ). Several trial runs were performed to minimize the error. Experiments were repeated for super saturations, such as 1.10, 1.15 and 1.20 at two different temperatures.

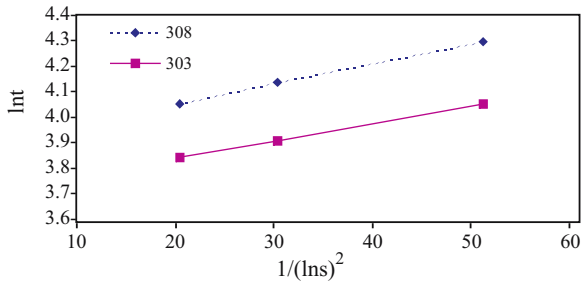

Fig. 5 A plot of ln*t vs.* $1/(\ln s)^2$ for benzophenone in $CHCl_3$

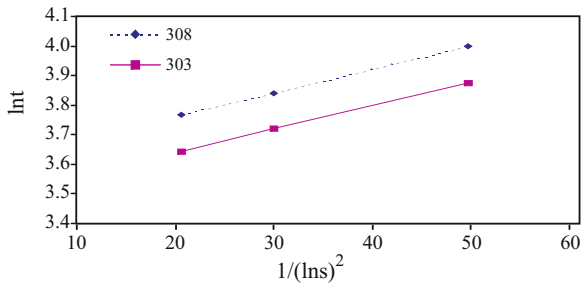

Fig. 6 A plot of ln*t vs.* $1/(\ln s)^2$ for benzophenone in CCl_4

From the results obtained, a plot of $\ln\tau$ *vs.* $1/(\ln S)^2$ is drawn and shown in Fig. 5. The interfacial tension was calculated from the slope of the curves using the equation

$$\ln\tau=\ln A+16\pi\gamma^3V^2N/3RT(\ln S)^2 \quad (1)$$

where A is a constant related to the pre-exponential factor of the nucleation rate expression, V is the molar volume, N is the Avagadro number and R is the gas constant. The factor $16\pi/3$ in the above equation refers to the spherical nuclei. The interfacial tension between the benzophenone and $CHCl_3$ is calculated by measuring the slope value of the curve obtained at two temperatures. The similar experiment was also carried out in CCl_4 solvent. From the results obtained, a plot of $\ln\tau$ *vs.* $1/(\ln S)^2$ is drawn and shown in Fig. 6. The effect of solvent and temperature on interfacial tension is presented in Table 3.

Table 3 Effect of temperature and solvent on interfacial tension

Solvent	Temperature/ °C	Slope value	Interfacial tension/mJ m^{-2}
$CHCl_3$	30	$8.33\cdot10^{-3}$	1.218
	35	$8.57\cdot10^{-3}$	1.237
CCl_4	30	$9.23\cdot10^{-3}$	1.261
	35	$9.33\cdot10^{-3}$	1.272

According to the classical homogenous nucleation theory, the free energy required to form anthracene nucleus is given by

$$\Delta G=(4/3)\pi r^3\Delta G_v+4\pi r^2\gamma \quad (2)$$

where ΔG_v is the energy change per unit volume, r is radius of the nucleus. At the critical state, the free energy of formation obeys the condition that $d(\Delta G)/dr=0$. Hence the radius of the critical nucleus is expressed as

$$r^*=-2\gamma/\Delta G_v$$

where

$$\Delta G_v=-KT\ln S/V \quad (3)$$

where V in the molar volume, and $S=C/C^*$, C – actual concentration and C^* – equilibrium concentration. Hence

$$r^*=2V\gamma/KT\ln S \quad (4)$$

The critical free energy is given by

$$\Delta G^*=16\ \pi\gamma^3V^2/\Delta G_v^2 \quad (5)$$

The number of molecules in the critical nucleus is expressed as

$$i^*=4\pi(\gamma^*)^3/3V \quad (6)$$

Therefore, using the interfacial tension value, the radius of the critical nuclei (r^*), the free energy change for the formation of a critical nucleus (ΔG^*) and the number of molecules in the critical nucleus (i^*) were calculated at two different temperatures for benzophenone in $CHCl_3$, and presented in Table 4.

It was noted that with the increase in super saturation, the free energy change for the formation of a critical nucleus (ΔG^*) decreases with radius (r^*). This favors the easy formation of nucleation in $CHCl_3$ solutions at higher super saturations.

Similar type of calculations used to calculate the nucleation parameters of benzophenone in CCl_4 and the values are given in Table 5.

Table 4 Nucleation parameters of benzophenone crystal in $CHCl_3$

Super saturation ratio $S=C/C^*$	30°C			35°C		
	r^*	(ΔG^*)	i^*	r^*	(ΔG^*)	i^*
	10^{11} m	10^{13} kJ	10^{38}	10^{11} m	10^{13} kJ	10^{38}
1.10	13.68	4.806	4.788	13.67	4.866	4.778
1.15	9.34	2.239	1.524	9.33	2.268	1.519
1.20	7.15	1.313	0.683	7.14	1.329	0.680

Table 5 Nucleation parameters of benzophenone crystal in CCl_4

Super saturation ratio $S=C/C^*$	30°C			35°C		
	r^*	(ΔG^*)	i^*	r^*	(ΔG^*)	i^*
	10^{11} m	10^{13} kJ	10^{38}	10^{11} m	10^{13} kJ	10^{38}
1.10	14.16	5.323	5.310	14.06	5.295	5.199
1.15	9.67	2.480	1.691	9.60	2.468	1.654
1.20	7.40	1.454	0.757	7.35	1.446	0.742

Table 6 Effect of surface tension of solvents on interfacial tension

Solvent	Surface tension at 20°C/mJ m^{-2}	Interfacial tension at 30°C/mJ m^{-2}
$CHCl_3$	27.14	1.218
CCl_4	27.0	1.261

The effect of surface tension of solvents on interfacial tension of benzophenone is given in Table 6. It can be concluded from the results that as the surface tension decreases, the interfacial tension increases. The effect of viscosity of solvents on interfacial tension is given in Table 7. As viscosity increases the interfacial tension also increases. The effect of density of solvents on interfacial tension is given in Table 8. As density of solvent increases, the interfacial tension also increases.

Measurements

The FTIR spectrum of solution grown benzophenone was recorded between 400–4000 cm^{-1} using KBr pellet technique.

The SHG efficiency of benzophenone was tested by using Nd:YAG laser source.

The ^{1}HNMR spectrum recorded for the benzophenone in $CDCl_3$ at 400 MHz in JEOL instrument.

UV visible spectrophotometer (Version 02.00) was used to record the UV visible spectrum of the grown crystals.

Table 7 Effect of viscosity of solvents on interfacial tension

Solvent	Viscosity	Interfacial tension at 30°C/mJ m^{-2}
$CHCl_3$	0.518	1.218
CCl_4	0.845	1.261

Table 8 Effect of density of solvents on interfacial tension

Solvent	Density/g mL^{-1}	Interfacial tension at 30°C/mJ m^{-2}
$CHCl_3$	1.4985	1.218
CCl_4	1.6320	1.261

The high resolution GUINIER powder X-ray diffractometer (CSEIFERT, Germany) with CuK_α radiation has been used for X-ray diffraction studies.

Results and discussion

FTIR spectral analysis

The characteristic FTIR spectral peak of solution grown benzophenone at 1650 cm^{-1} is assigned to C=O. The aromatic skeletal vibrations are assigned to peak at 1447 cm^{-1}. The C–H deformation vibration is assigned to 935 cm^{-1}. Thus the FTIR spectrum of harvested crystals is in good agreement with the standard values.

UV-Visible spectral analysis

The UV spectrum provides information recording the functional groups and transparency of the grown benzophenone. The UV spectrum of benzophenone is shown in Fig. 7. Since it is a colourless crystal no absorption is found between 400–800 nm. The maximum absorption bands at 347 and 248 nm are characteristic peaks of C=O and aromatic ring. It is transparent between 600–1000 nm, which is an important requirement to a material for NLO properties.

NLO property

The SHG signal of benzophenone was found to be 96. It indicates that the SHG efficiency of benzophenone

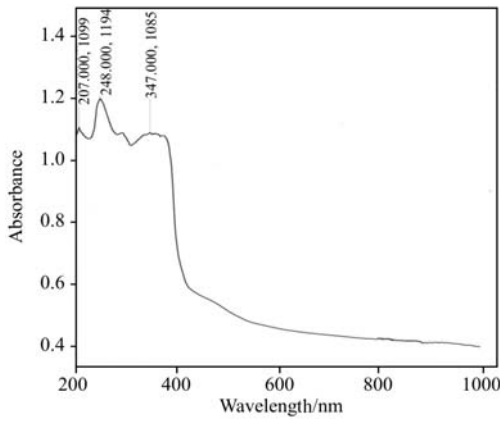

Fig. 7 UV absorbance spectrum of benzophenone

is 96/149.5=0.64, which means benzophenone is 0.64 times SHG efficient than KDP crystals. Nd:YAG laser of fundamental wavelength 1064 nm, was allowed to focused on capillary densely packed with the sample. The signal was collected at 90 deg to the incident beam using aczerny turner monochromator and a visible photomultiplier tube (Hamamatsu R2059) and recorded in a digital storage oscilloscope (Tektronix TDS 3000B).

^{1}HNMR spectral analysis

The ^{1}HNMR spectrum of the benzophenone in $CDCl_3$ showed multiplet of 14 peaks in the aromatic region. All the ten protons of two phenyl rings are present in the deshielding region of both the carbonyl group and the benzene ring, which is shown in Fig. 8. Here the two phenyl rings and the carbonyl group are in a same plane and hence all the protons are neighbouring. Radio frequency in the down field region is observed between 7.2476 and 7.8448. If there is any deviation from the planarity, a few protons of one phenyl ring may go to the shielding region of other benzene ring and vice versa and show low delta value [67].

Powder XRD studies

Powder X-ray diffraction patterns of benzophenone are shown in Fig. 9. Most of the lattice parameters evaluated by powder XRD studies of solution grown benzophenone are in good agreement with the literature data. The photograph of solution grown benzophenone also indicates the hexagonal structure. Further, the narrow and strongest peak along the (021) direction confirms the single crystalline nature of the solution grown benzophenone.

Thermal studies

Differential thermal analysis (DTA) and thermogravimetric analysis (TG) were carried out on the crystal samples for qualitative analysis. These studies were conducted for solution grown benzophenone

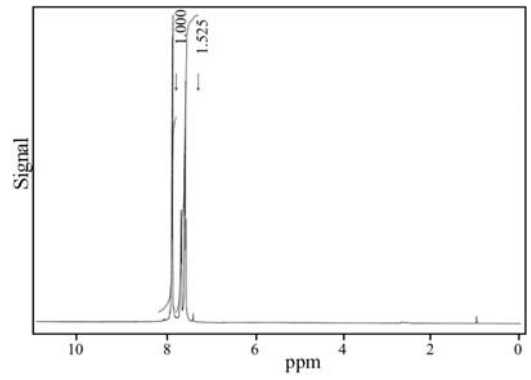

Fig. 8 ^{1}HNMR spectrum of solution grown benzophenone

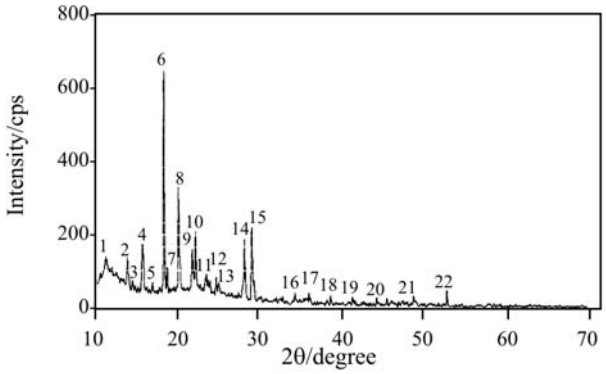

Fig. 9 XRD pattern of benzophenone

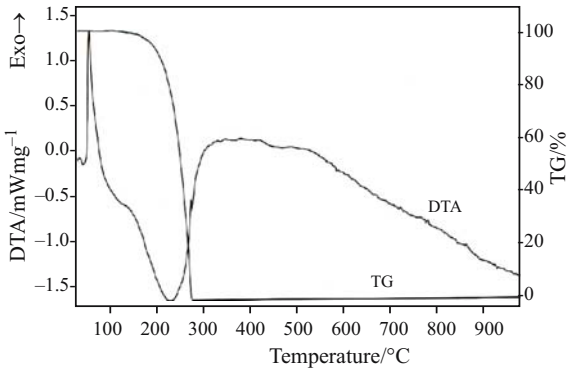

Fig. 10 TG and DTA curves of solution grown benzophenone

crystals. Both TG and DTA were carried out simultaneously. The mass change in the sample with temperature was studied by TG and the energy change in the sample on temperature was studied by DTA. The analysis was performed in nitrogen atmosphere at heating rate of 10°C min^{-1}.

The TG and DTA curves for the decomposition of benzophenone are shown in Fig. 10. The TG curve indicates that it is thermally stable up to 160°C. Afterwards, the TG curve shows an intense single step mass loss at 160–273°C corresponding to the decomposition of benzophenone. The DTA curve for benzophenone (Fig. 10) shows an intensive exothermic peak at 49°C due to the melting of benzophenone and an intensive endothermic peak at 225°C ascribed to the decomposition of benzophenone.

Conclusions

Benzophenone was grown by simple solution technique adopting slow evaporation method from $CHCl_3$ and CCl_4. Induction period and interfacial tension of benzophenone in $CHCl_3$ and CCl_4 were determined at different super saturation ratios such as 1.10, 1.15, 1.20 and 1.25 at 303 and 308 K. Using induction period and interfacial tension, nucleation parameters were calculated, interfacial tension was

correlated with surface tension, viscosity, density of the solvents.

UV absorbance spectrum provides information about the transparency of the grown crystals. It is transparent between 400–1200 nm with about 99% transmission. FTIR spectrum provides information about the presence of C=O functional group in benzophenone. ^{1}HNMR confirms the structure of the benzophenone and shows there is no solvent inclusion in the grown crystals. In the X-ray diffraction pattern of grown benzophenone crystals, there is a strong, narrow peak along the (021) direction, which shows the single crystalline nature of the grown crystals. NLO studies show that the grown benzophenone crystal is found to be 0.64 times SHG efficient than KDP crystals.

References

1 J. Badan, R. Hierle, A. Perigaud and J. Zyss, Acs Symp., 233 (1983) 81.
2 D. S. Chemla and J. Zyss (Eds), Nonlinear Optional Properties of Organic Molecules and Crystals, Vol. 1, 2, Academic press, New York (1987).
3 A. F. Garito and K. D. Singer, Laser Focus Fiber Opt. Technol., 18 (1982) 59.
4 J. Bleay, R. M. Hooper, R. S. Narang and J. N. Sherwood, J. Cryst. Growth, 43 (1978) 589.
5 T. Scheften-Lauenroth, R. A. Becker and H. Klapper, Kristallogr., 167 (1984) 159.
6 K. Katoh and N. Kato, J. Cryst. Growth, 73 (1985) 203.
7 M. Tachibana, S. Motomura, A. U. Qitang and K. Kojima, Jpn. J. Appl. Phys., 31 (1992) 2202.
8 R. M. Hooper, B. J. McArdle, R. S. Narang and J. N. Sherwood, Crystal Growth, Eds, B. Pamplin (Pergamon Press, Oxford 1980) p. 395.
9 B. J. McArdle and J. N. Sherwood, Adv. Crystal Growth, Eds P. M. Dryburgh, B. Cockayne and K. G. Bassaclough Prentice Hall, New York 1987.
10 P. Cockorham, C. C. Frazier, S. Guha and E. A. Chauchard, Appl. Phys., B53 (1991) 275.
11 D. Lammers, K. Betzler, D. Xue and J. Zhao, Phys. Stat. Sol., 180 (2000) R5.
12 D. Czakis-Sulikowska, A. Czylkowska and A. Malinowska, J. Therm. Anal. Cal., 67 (2002) 667.
13 E. Jóna, M. Kubranová, P. Šimon and J. Mroziński, J. Thermal Anal., 46 (1996) 1325.
14 E. Jóna, A. Sirota, P. Šimon and M. Kubranová, Thermochim. Acta, 258 (1995) 161.
15 A. Ramadevi and K. Srinivasan, Res. J. Chem. Environ., 9 (2005) 54.
16 K. Kundu and M. A. H. Miah, Jahangirnagar Univ. J. Sci., 19 (1995) 49.
17 M. Enamullah and W. Linert, J. Coord. Chem., 35 (1995) 325.
18 R. N. Patel and K. B. Pandeya, Synth. React. Inorg. Met.-Org. Chem., 28 (1998) 23.
19 J. S. Skoršepa, K. Györyová and M. Melník, J. Thermal Anal., 44 (1995) 169.
20 R. N. Patel and K. B. Pandeya, J. Inorg. Biochem., 72 (1998) 109.
21 D. Ondrušová, E. Jóna and P. Šimon, J. Therm. Anal. Cal., 67 (2002) 147.
22 E. Jóna, E. Rudinska, M. Sapietova, M. Pajtášová and D. Ondrušová, Res. J. Chem. Environ., 10 (2006) 31.
23 M. Pajtášová, E. Jóna, M. Koman and D. Ondrušová, Pol. J. Chem., 75 (2001) 1209.
24 E. Jóna, M. Pajtášová, D. Ondrušová and P. Šimon, J. Anal. Appl. Pyrol., 63 (2002) 17.
25 M. Kubranová, E. Jóna, E. Rudinská, K. Nemčeková, D. Ondrušová and M. Pajtášová, J. Therm. Anal. Cal., 74 (2003) 251.
26 E. Jóna, M. Hvastijová and J. Kohout, J. Thermal Anal., 41 (1994) 161.
27 G. D'Ascenzo, U. B. Ceipidor, E. Cardarelli and A. D. Magri, Thermochim. Acta, 13 (1975) 449.
28 E. A. Ukraintseva, V. A. Logvinenko, D. V. Soldatov and T. A. Chingina, J. Therm. Anal. Cal., 75 (2004) 337.
29 B. R. Srinivasan and S. C. Sawant, Thermochim. Acta, 402 (2003) 45.
30 D. Czakis-Sulikowska and A. Czylkowska, J. Therm. Anal. Cal., 71 (2003) 395.
31 E. Jóna and M. Jamnický, J. Thermal Anal., 27 (1983) 359.
32 M. Melník, M. Koman and T. Glowiak, Polyhedron, 17 (1998) 1767.
33 E. Jóna, T. Šramko and J. Gažo, J. Thermal Anal., 16 (1979) 213.
34 A. Krutošíková, B. Mitasová, E. Jóna and M. Bobošíková, Chem. Papers, 55 (2001) 290.
35 M. Melník, I. Potočnak, L. Macášková and D. Mikloš, Polyhedron, 15 (1996) 2159 and refs therein.
36 S. Cakir, I. Bulut, E. Bicer, E. Coskun and O. Cakir, J. Electroanal. Chem., 511 (2001) 94.
37 D. Czakis-Sulikowska, A. Czylkowska, A. Malinowska, J. Therm. Anal. Cal., 65 (2001) 505.
38 S. C. Mojumdar, M. Melník and E. Jóna, J. Anal. Appl. Pyrol., 46 (1998) 147.
39 S. C. Mojumdar, M. Melník and E. Jóna, Pol. J. Chem., 73 (1999) 293.
40 S. C. Mojumdar, M. Valko and M. Melník, Chem. Papers, 52 (1998) 650.
41 S. C. Mojumdar, M. Melník and M. Valko, Pol. J. Chem., 73 (1999) 457.
42 S. C. Mojumdar, M. Melník and E. Jóna, J. Anal. Appl. Pyrol., 48 (1999) 111.
43 S. C. Mojumdar, M. Melník and E. Jóna, Thermochim. Acta, 352 (2000) 129.
44 S. C. Mojumdar, D. Hudecová and M. Melník, Pol. J. Chem., 73 (1999) 759.
45 S. C. Mojumdar, M. Melník and E. Jóna, J. Therm. Anal. Cal., 56 (1999) 533.
46 S. C. Mojumdar, L. Martiška, D. Valigura and M. Melník, J. Therm. Anal. Cal., 74 (2003) 905.
47 S. C. Mojumdar, M. Melník and E. Jóna, J. Therm. Anal. Cal., 56 (1999) 541.
48 S. C. Mojumdar, M. Melník and E. Jóna, J. Anal. Appl. Pyrol., 53 (2000) 149.
49 S. C. Mojumdar, K. Lebrušková and D. Valigura, Chem. Papers, 57 (2003) 245.
50 S. C. Mojumdar, I. Ondrejkovičová, L. Nevid'anská and M. Melník, J. Anal. Appl. Pyrolysis, 64 (2002) 59.

51 S. C. Mojumdar, M. Melník and M. Valko, Pol. J. Chem., 73 (1999) 457.
52 M. Melník, S. C. Mojumdar and M. Koman, Pol. J. Chem., 73 (1999) 1293.
53 M. T. Saleh, S. C. Mojumdar and M. Lamoureux, Res. J. Chem. Environ., 10 (2006) 14.
54 S. C. Mojumdar, K. G. Varshney, P. Gupta and A. Agrawal, Res. J. Chem. Environ., 10 (2006) 85.
55 S. C. Mojumdar, K. G. Varshney and A. Agrawal, Res. J. Chem. Environ., 10 (2006) 89.
56 S. C. Mojumdar, G. Madhurambal and M. T. Saleh, J. Therm. Anal. Cal., 81 (2005) 205.
57 K. G. Varshney, A. Agrawal and S. C. Mojumdar, J. Therm. Anal. Cal., 81 (2005) 183.
58 E. Jóna, E. Rudinská, M. Sapietová, M. Pajtášová, D. Ondrušová, V. Jorík and S. C. Mojumdar, Res. J. Chem. Environ., 9 (2005) 41.
59 S. C. Mojumdar, L. Martiška, D. Valigura and M. Melník, J. Therm. Anal. Cal., 81 (2005) 243.
60 S. C. Mojumdar, J. Miklovic, A. Krutošíková, D. Valigura and J. M. Stewart, J. Therm. Anal. Cal., 81 (2005) 211.
61 S. C. Mojumdar, Res. J. Chem. Environ., 9 (2005) 23.
62 G. Madhurambal, S. C. Mojumdar, S. Hariharan and P. Ramasamy, J. Therm. Anal. Cal., 78 (2004) 125.
63 S. C. Mojumdar, J. Therm. Anal. Cal., 64 (2001) 629.
64 S.C. Mojumdar and M. Melník, Chem. Pap., 54 (2000) 1.
65 G. Madhurambal, P. Ramasamy, P. A. Srinivasan and S. C. Mojumdar, J. Therm. Anal. Cal., in press (2006).
66 M. Arivanandhan, K. Sankaranarayanan, K. Ramamoorthy C. Sanjeeviraja and P. Ramasamy, Cryst. Res. Technol., 39 (2004) 692.
67 P. Kalsi, Spectroscopy of Organic Compounds, Wiley Eastern, New Delhi, 1985.

DOI: 10.1007/s10973-007-8521-x